Hydrol. Earth Syst. Sci. Discuss., doi:10.5194/hess-2016-194, 2016
Manuscript under review for journal Hydrol. Earth Syst. Sci.
Published: 9 May 2016

Hydrology and Earth System Sciences
Open Access
Discussions

Application of runoff coefficient and rainfall-intensity-ratio to analyze the relationship between storm patterns and flood responses

Nam Won Kim [1], Mun-Ju Shin [1]*, Jeong Eun Lee [1]

[1] Water Resources & River Research Institute, Korea Institute of Civil Engineering and Building Technology, 283, Goyangdae-ro, Ilsanseo-gu, Goyang-si, Gyeonggi-do, 411-712, Republic of Korea

Nam Won Kim: nwkim@kict.re.kr (ph: +82 (0) 31 9100 256)
Jeong Eun Lee: jeus22@kict.re.kr (ph: +82 (0) 31 9100 275)
* Correspondence to: Mun-Ju Shin: mjshin@kict.re.kr (ph: +82 (0)31 9100 475; Fax: +82 (0)31 9100 251)

Hydrol. Earth Syst. Sci. Discuss., doi:10.5194/hess-2016-194, 2016
Manuscript under review for journal Hydrol. Earth Syst. Sci.
Published: 9 May 2016

Hydrology and Earth System Sciences
Open Access
Discussions

Abstract

The analysis of the effects of storms on floods is essential for designing hydraulic structures and flood plains. Observations of the flow time series for the various catchment sizes are needed to understand the effects on floods, but it is not easy to obtain these datasets because most stream channels are ungauged. Hence, a reasonable method for generating the flow time series for the ungauged catchments is needed to secure the datasets. A quantitative analysis for investigating the relationship between the natural storm patterns, the peak flows, the volumes of floods, and their durations for the various catchment sizes is also needed. This study suggests a method to investigate quantitatively the relationship between storms and floods using datasets generated for the ungauged catchments. The relationship between the runoff coefficients and the rainfall-intensity-ratios with respect to catchment sizes for the dependent catchments showed that the events can be separated into four physically reasonable types using the pattern of storms and flood responses. This indicates that the relationship between the pattern of storms and flood responses for any event in terms of dependent catchments can be analyzed using plots of runoff coefficients and rainfall-intensity-ratios versus the catchment size. There are correlations between the runoff coefficients and the rainfall-intensity-ratios for the independent catchments, but these correlations have no relationship with the four types of events from the dependent catchments.

Key Words: flood-intensity-duration curve, time of concentration, spatial data extension, storm pattern, distributed model

Hydrol. Earth Syst. Sci. Discuss., doi:10.5194/hess-2016-194, 2016
Manuscript under review for journal Hydrol. Earth Syst. Sci.
Published: 9 May 2016

1 Introduction

The analysis of the effect of rainfall on flow responses is an essential step in understanding natural hydrological phenomena. There are various studies that analyze the effect of rainfall (e.g., the rain gauge density, the spatial rainfall variability, the rainfall disaggregation, and the rainfall grid resolution) on flow responses, the relationship between storms and catchment scale, and the uncertainty analysis of rainfall error or temporal variability of rainfall on flow responses (Wood et al., 1988; Woolhiser and Goodrich, 1988; Kuczera and Williams, 1992; Duncan et al., 1993; Michaud and Sorooshian, 1994; Bronstert and Bárdossy, 2003; Smith et al., 2004; Chaplot et al., 2005; Schuurmans and Bierkens, 2007; Vischel and Lebel, 2007; Vischel et al., 2009; Xu et al., 2013; Zhao et al., 2013). Many studies, especially those on the effects of storms on flood responses have used short time series and catchments smaller than ~100 km^2 (Faurès et al., 1995; Shah et al., 1996; Bell and Moore, 2000; Syed et al., 2003; Anquetin et al., 2010; Moreno et al., 2012). Observed flow time series for the various catchment sizes are needed to fully understand the storm effects on floods, but it is not easy to get these datasets because most stream channels are ungauged. Therefore, a reasonable method for generating the flow time series for the ungauged catchments is needed (Tewolde and Smithers, 2007, Smith et al., 2012). There are many studies for calibrating the model parameters to calculate the flood time series for the ungauged catchments by statistical methods using the catchment characteristics and the model parameters for gauged catchments (Bhaskar et al., 1997; Takeuchi and Ishidaira,1999; Dawson et al., 2006; Goswami et al., 2007; Reed et al., 2007; Mapiam and Sriwongsitanon, 2009; Viviroli et al., 2009), but most of them are for the estimation of flood time series with a daily time step or for estimation of the flood peak only. Oudin et al. (2010) argued that physical similarity does not guarantee hydrological similarity. Therefore, a reasonable method with good applicability is needed to generate the flood time series for the ungauged catchments.

Storm patterns based on the spatial and temporal variability of precipitation affect not only peak flow but also flood volume and duration for the various catchment sizes and are

Hydrol. Earth Syst. Sci. Discuss., doi:10.5194/hess-2016-194, 2016
Manuscript under review for journal Hydrol. Earth Syst. Sci.
Published: 9 May 2016

important in the design of hydraulic structures or in mapping flood plains (Javelle et al., 2002). Various studies have investigated the effects of storms on the peak flow and/or flood volume, including an investigation of the relationship between various catchment sizes from small to large area and the annual maximum flow (Cannarozzo et al., 1995), an investigation of the relationship between storm movement over a short period (2 h) and flood volume for hypothetical small catchments (from 0.5 km^2 to 32 km^2) (Sargent 1981, 1982), an investigation of the impact of higher-resolution spatial rainfall with spatial variability on streamflow generation (Lobligeois et al., 2014), and an investigation of the variability of artificial storms with short or long periods on hydrographs or peak flow and flood volume for various catchment sizes covering small to large areas (Krajewski et al., 1991; Ogden and Julien, 1993; Obled et al., 1994; Faurès et al., 1995; Arnaud et al., 2002; Saulnier and Le Lay, 2009; Huang et al., 2011; Paschalis et al., 2014). However, there are not enough studies that analyze the storm effects on floods quantitatively, using the factors extracted from the times series of various patterns of natural storms and floods for the various sizes of natural catchments that cover small to large areas. Therefore, an additional method is needed for the quantitative analysis of the relationship between storms and floods.

This study suggests new techniques that are data generation technique for the ungauged catchments to secure sufficient data, and an analysis technique using time of concentration (TC) to investigate the relationship between storm types and flood responses. A simple data generation method generates the hourly flood time series for the ungauged catchments of interest by the simulation of a distributed rainfall-runoff model using the parameters calibrated from the gauged catchments. More details for this method are described in Sect. 3.1.

Time of concentration is the time of flow from the most distant point in the catchment to the outlet (Chow et al., 1988). The TC can be used as an important measure when investigating the storm effects on flood responses (Nicótina et al., 2008). Alexander (1972) investigated the relationships between the rainfall intensity and the flood intensity and between the flood intensity and catchment sizes, but he did not use the TC for the analysis.

Hydrol. Earth Syst. Sci. Discuss., doi:10.5194/hess-2016-194, 2016
Manuscript under review for journal Hydrol. Earth Syst. Sci.
Published: 9 May 2016

94 For this study, we calculate the runoff coefficients and the rainfall-intensity-ratios using TC
95 and the time series of areal rainfall and floods for gauged and ungauged catchments. The
96 relationship between the pattern of storms and flood responses was then analyzed
97 quantitatively using the factors of runoff coefficients and rainfall-intensity-ratios. This study,
98 therefore, was based on studies that have argued that the characteristics of storms drive the
99 flood responses (Singh, 1997; Segond et al., 2007; Nicótina et al., 2008; Zoccatelli et al., 2010).
100 We analyzed this for both dependent catchments and independent catchments. More details
101 are described in Sects. 3.3 - 3.5.
102 Section 2 describes the catchments, the input data, the objective function for parameter
103 calibration, and the distributed rainfall-runoff model. Section 3 describes the methods used,
104 and Sect. 4 gives the results. Discussion and conclusions are in Sect. 5.
105

106 **2 Catchments, Input Data, Objective Function, and Rainfall-Runoff Model**

107 2.1 Catchments

108 The study area is the Andongdam catchment (1,584 km^2), which is a mountainous
109 catchment located in the eastern part of the Republic of Korea (Fig. 1). This catchment is
110 important for reducing flood damage and in securing water for agriculture, industry, and
111 domestic use. We selected three gauged catchments with water level gauging points
112 (Andongdam, Dosan, and Socheon) at the outlets to use the observed flow for the calibration
113 and validation of the parameters of the distributed rainfall-runoff model that will be
114 described in Sect. 2.4. An additional 47 ungauged catchments were selected to investigate
115 the storm effects on floods covering a range in catchment sizes. The information from the
116 gauged and ungauged catchments is in Table A1, while the method of selection of the
117 ungauged catchments is described in Sect. 3.1.

118 2.2 Input Data

Hydrol. Earth Syst. Sci. Discuss., doi:10.5194/hess-2016-194, 2016
Manuscript under review for journal Hydrol. Earth Syst. Sci.
Published: 9 May 2016

For input rainfall data for the flood simulation, we used the hourly time step rainfall data (Korea Meteorological Administration (http://www.kma.go.kr/), Ministry of Land, Infrastructure and Transport (www.molit.go.kr), and K-water (www.kwater.or.kr)) from up to 27 rainfall gauge stations that are located within and near the Andongdam catchment. Data from 20 events were extracted from 1998 to 2009 period (Table A2). These datasets have relatively large magnitude and long duration of precipitation covered the entire catchments that reflect the monsoon climate in the Republic of Korea. The grid rainfall datasets (resolution 200×200 m^2) were generated for the input of the distributed rainfall-runoff model by an ordinary kriging method using the point rainfall data. Therefore, the distributed rainfall-runoff model considers the spatial and temporal variability of precipitation.

For the observed flow from the three water level gauge points during the 20 events, we used the data related to water level and rating from the Water Resources Management Information System (www.wamis.go.kr).

A Digital Elevation Model (DEM), a soil map, and a land use map were used for the distributed model simulation. The scales of these data are 1:25,000. The grid data of the DEM, soil map, and land use map were generated with the resolution of 200×200 m^2, which were used as the input of the distributed rainfall-runoff model. Therefore, the distributed rainfall-runoff model considers the spatial variability of the geophysical catchment characteristics.

2.3 Objective Function and Performance Evaluation Statistics

The Nash-Sutcliffe Efficiency (NSE) (Nash and Sutcliffe, 1970), which has been widely used in rainfall-runoff modelling, was used as an objective function for the parameter calibration.

$$NSE = 1 - \frac{\sum_{i=1}^{n}\left(Q_{obs,i} - Q_{sim,i}\right)^2}{\sum_{i=1}^{n}\left(Q_{obs,i} - \overline{Q_{obs}}\right)^2} \quad (1)$$

Hydrol. Earth Syst. Sci. Discuss., doi:10.5194/hess-2016-194, 2016
Manuscript under review for journal Hydrol. Earth Syst. Sci.
Published: 9 May 2016

Hydrology and Earth System Sciences
Discussions

where n is the total number of time steps, $Q_{obs,i}$ is the observed flow at the time step *i* (hourly), $\overline{Q_{obs}}$ is the mean of the observed flow, and $Q_{sim,i}$ is the simulated flow. The range of NSE is [-∞, 1], where unity means that the rainfall-runoff model simulated the observed flow perfectly.

Legates and McCabe (1999) and Krause et al. (2005) mentioned that the NSE emphasizes the high flow fitting because of the squared differences between the observed and simulated values, and this is the drawback of the NSE because low flow fitting is neglected. This study, however, can use the NSE as an objective function because of focusing on fitting flood hydrograph only.

Three quantitative statistics were used to evaluate the model performance: NSE, percent bias (PBIAS), and modified correlation coefficient (r_{mod}) (McCuen and Snyder, 1975). We selected the NSE because it is a recommended performance statistic for use by ASCE (1993) and provides the overall information on simulated values (Moriasi et al., 2007).

The PBIAS calculates the total volume difference between simulated and observed flow time series, which is expressed as a percentage. The best PBIAS value is zero, and lower magnitude values of PBIAS represent more accurate model performances. The positive PBIAS values indicate overestimation of simulated flows. We selected the PBIAS because it is recommended by Smith et al., (2004) as an important measure to evaluate the simulated flows, and it indicates the poor model performance clearly in terms of volume of simulated flow (Gupta et al., 1999).

$$PBIAS = \frac{\sum_{i=1}^{n}\left(Q_{sim,i} - Q_{obs,i}\right)}{\sum_{i=1}^{n} Q_{obs,i}} \times (100) \quad (2)$$

Moriasi et al. (2007) recommended the use of NSE, PBIAS, and ratio of the root mean square error to the standard deviation of measured data (RSR) for the evaluation of the model simulation performances. However, the RSR has similar form to the NSE therefore, we selected the r_{mod} instead because it is a useful performance statistic for the model evaluation, which is demonstrated by the study of Smith et al. (2012). The r_{mod} is the

Hydrol. Earth Syst. Sci. Discuss., doi:10.5194/hess-2016-194, 2016
Manuscript under review for journal Hydrol. Earth Syst. Sci.
Published: 9 May 2016

Hydrology and Earth System Sciences
Discussions

correlation coefficient adjusted by a ratio of minimum standard deviation to maximum standard deviation among the simulated and observed flows to evade the significant influence from outliers and the insensitivity to the differences in volumes within the correlation coefficient (McCuen and Snyder, 1975). The correlation coefficient is defined as:

$$r = \frac{n\sum_{i=1}^{n} Q_{sim,i}Q_{obs,i} - \sum_{i=1}^{n} Q_{sim,i}\sum_{i=1}^{n} Q_{obs,i}}{\sqrt{\left[n\sum_{i=1}^{n} Q_{sim,i}{}^{2} - \left(\sum_{i=1}^{n} Q_{sim,i}\right)^{2}\right]\left[n\sum_{i=1}^{n} Q_{obs,i}{}^{2} - \left(\sum_{i=1}^{n} Q_{obs,i}\right)^{2}\right]}} \quad (3)$$

The standard deviations for simulated and observed flow are defined as:

$$\sigma_{sim} = \sqrt{\frac{\sum_{i=1}^{n}\left(Q_{sim,i} - \overline{Q_{sim}}\right)^{2}}{n-1}} \quad (4)$$

$$\sigma_{obs} = \sqrt{\frac{\sum_{i=1}^{n}\left(Q_{obs,i} - \overline{Q_{obs}}\right)^{2}}{n-1}} \quad (5)$$

The modified correlation coefficient is defined as:

$$r_{\mathrm{mod}} = r \times \frac{\min\{\sigma_{sim}, \sigma_{obs}\}}{\max\{\sigma_{sim}, \sigma_{obs}\}} \quad (6)$$

The satisfactory model performance statistics in this study are: NSE > 0.5 (Moriasi et al., 2007), PBIAS±30%, and r_{mod} > 0.6. Moriasi et al. (2007) suggested the PBIAS±25% for the monthly streamflow simulations, which tend to have better model performances due to smoothing the flow values compare to the daily or hourly simulations. Therefore we slightly extend the width of range for the PBIAS by ±5% considering this tendency. This extension of PBIAS range is reasonable from the results of Smith et al. (2012), which has the PBIAS values without the outliers within this extended range for the calibration periods using the various rainfall-runoff models including conceptual and distributed models. The satisfactory range of r_{mod} is selected from the study of Smith et al. (2012), which showed that the most r_{mod} values were placed in more than 0.6 r_{mod} for the calibration period, modeled by the aforementioned various rainfall-runoff models.

2.4 Grid Based Rainfall-Runoff Model

Hydrol. Earth Syst. Sci. Discuss., doi:10.5194/hess-2016-194, 2016
Manuscript under review for journal Hydrol. Earth Syst. Sci.
Published: 9 May 2016

This study used a Grid based Rainfall-runoff Model (GRM) (Choi et al., 2015), which is a physically-based distributed rainfall-runoff model with hourly time step. This model simulates the surface flow, the infiltration, the subsurface flow, the baseflow, and the impact of the flow control facilities. The surface flow is composed of the overland flow and the channel flow that are calculated by a kinematic wave model. The GRM model uses the upper and the lower soil layers to calculate the infiltration, the subsurface flow, and the baseflow. The upper soil layer is used to calculate the infiltration and the subsurface flow, and the lower soil layer is used to calculate the baseflow. The Green–Ampt model is used to calculate the infiltration. The kinematic wave model calculates the subsurface flow based on the hypothesis that the hydraulic gradient in the control volume is equal to the ground surface slope for the saturated zone (Beven, 1981). The water percolates from the upper to the lower soil layer when the upper soil layer is saturated. Darcy's law calculates the lateral flow from the baseflow in the lower soil layer (Freeze and Cherry, 1979). More details of the GRM model are described in Choi et al. (2015). The GRM model has 12 parameters (Table 1). The ranges of parameters were suggested by Choi (personal communication, 2016). The grid resolution for this study was 200 x 200 m^2, which satisfied the requirement of Bathurst (1986) that the grid area should be less than 1% of the catchment area.

The parameters that are calibrated are Nos. 1 to 5 in Table 1. The calibrated values of the parameter No. 1 are different for different events because every event begins with different initial soil moistures. The parameters from Nos. 2 to 5 are about the catchment characteristics that should have consistent values for the physically-based distributed model regardless of rainfall in flood events. The calibration procedure will be described in Sect. 3.1. The observed initial flows at the Andongdam water level gauge point were used for the parameter No. 6. We used the default value of zero for the parameter No. 7, and the default value of one for the parameters Nos. 8 to 12 due to using the original catchment characteristics from the DEM, the land cover, and the soil type data.

3 Method

Hydrol. Earth Syst. Sci. Discuss., doi:10.5194/hess-2016-194, 2016
Manuscript under review for journal Hydrol. Earth Syst. Sci.
Published: 9 May 2016

220 3.1 Spatial Data Extension (SDE) Method

221 As mentioned in Sect. 1, the observed flow for small to large catchments are needed to
222 fully understand the natural hydrological responses, but there are many ungauged
223 catchments especially for the smaller upper catchments. We generated the flood time series
224 for the ungauged catchments in the Andongdam catchment by the Spatial Data Extension
225 (SDE) method suggested by this study.

226 The SDE method generates the flood time series of ungauged catchments by the GRM
227 model by applying the calibrated parameters from the gauged catchments. This method is
228 based on the hypothesis that if the simulated flow at the outlet by the distributed model is
229 the same as the observed flow then the simulated flow for each grid above the outlet is
230 reasonable because the simulated flow at the outlet is the aggregation of the routed flows of
231 all grids. Hence, this method can generate the simulated flow for any catchment of interest
232 by the distributed model. This idea can be extended to generate the simulated flow of the
233 ungauged catchment placed at downstream from the outlet. This method had the same key
234 idea as in the distributed model intercomparison project (DMIP) (Smith et al., 2012), which
235 hypothesized that the distributed models calibrated at the catchment outlet should produce
236 accurate simulation of hydrograph at interior ungauged catchments. However, there are
237 two differences between the SDE and the DMIP methods. Firstly, the DMIP method used
238 long term continuous hourly calibration at the outlet of the catchment. This long term
239 continuous hourly calibration has considerable computational burden therefore, it is
240 inefficient to produce hydrographs if the aim of the study is an investigation of floods only.
241 Whereas, the SDE method uses event calibration with hourly time step that takes much less
242 computational time, and this method can be applied to any distributed model including
243 event distributed models that are developed only for flood simulation purpose. Therefore,
244 the SDE method is more pragmatic for the modelers. Secondly, the DMIP method
245 calibrated at the outlet of the catchment and produced the flow at the interior ungauged
246 catchments. However, the SDE method can produce not only the flow at the interior

Hydrol. Earth Syst. Sci. Discuss., doi:10.5194/hess-2016-194, 2016
Manuscript under review for journal Hydrol. Earth Syst. Sci.
Published: 9 May 2016

ungauged catchments but also the one at the exterior ungauged catchments that are placed at the downstream from the gauged outlet.

The important idea of the SDE method is that the calibrated parameter values related to the geophysical catchment characteristics (parameters Nos. 2 to 5 in Table 1) should be reasonable for all of the events regardless of the storm characteristics in order to apply these parameter values to the ungauged catchments. This idea is reasonable because the geophysical catchment characteristics are the same regardless of the storm characteristics. Therefore, these parameters were calibrated for each event then the calibrated parameter sets were adjusted to get the same parameter values over all events by manual iteration, which had the possible best objective function values over all events. This adjustment process to get one optimal set of geophysical parameter values is named as parameter stabilization (PS) process in this study. The PS process had the similar key idea as in the regional calibration method (Parajka et al., 2007), which calibrated the parameters of the rainfall-runoff model for the many catchments simultaneously to get the same parameter values. Instead, the PS process calibrates the parameters of the rainfall-runoff model for the many events simultaneously to get the same parameter values. Note that the GRM model uses the geophysical input datasets as mentioned in Sect. 2.2 to consider geophysical spatial variability. The parameters in the GRM model related to the geophysical catchment characteristics are for setting the minimum thresholds or for select the channel roughness value that is not supplied from the geophysical input datasets. It is also worth to note that the purpose of the calibration by the SDE method is for generation of data for the ungauged catchments using all possible historical event datasets, which is not for the calibration of parameters for each or some event(s). Therefore, there are no validation periods for the split-sample test (Klemeš, 1986) in the SDE method.

After the calibration by the PS process for the geophysical parameters (first step of calibration), the parameter for initial soil saturation ratio (parameter No.1 in Table 1), which depends on antecedent soil moisture condition, is calibrated for each event that has the possible best objective function values (second step of calibration) therefore, the No. 1

Hydrol. Earth Syst. Sci. Discuss., doi:10.5194/hess-2016-194, 2016
Manuscript under review for journal Hydrol. Earth Syst. Sci.
Published: 9 May 2016

parameter has different values for different events because every event begins with different initial soil saturation ratio.

The two steps parameter calibration were applied to the calibration catchment, which is the Andongdam catchment (very lower catchment in Fig. 1), and the calibrated parameter sets were applied to the validation catchments, which are the Dosan and Socheon catchment (interior catchments) to verify the model performance. We assumed the validation catchments as the ungauged catchments for the purpose of generation of data for the ungauged catchments. Three performance evaluation statistics as mentioned in Sect. 2.3 were used for the calibration and validation catchments over the 20 events. If the ranges of the three performance evaluation statistics are similar and satisfactory for both the calibration and the validation catchments, they represents that the simulated flows for the validation/ungauged catchments can be generated by the SDE method with the similar magnitude of error in the simulated flows for the calibration catchment, which demonstrates the suitability of the SDE method. The result is shown in Sect. 4.1.

For the data generation for the ungauged catchments of interest, this study selected 47 additional points of interest (watch points, WP) in the Andongdam catchment and generated the 47 ungauged catchments using these points as the outlets (Fig. 1 and Table A1). We selected ungauged catchments that had various sizes ranging from small (5.6 km^2) to large (1459.7 km^2) to investigate the storm effects on flood responses for the various catchment sizes. Then the calibrated parameter values by the SDE method were applied to the 47 ungauged catchments to generate the flow time series data by the GRM model. We also calculated the flood time series for the three calibration and validation catchments, and areal rainfall time series for the 50 catchments by the GRM model for the analysis as described in Sect. 3.2.

3.2 Rainfall-Intensity-Duration Curve (RIDC) and Flood-Intensity-Duration Curve (FIDC)

We generated the Flood-Intensity-Duration Curve (FIDC) and the Rainfall-Intensity-Duration Curve (RIDC) by the Flood-Duration-Frequency (QDF) method (NERC, 1975; Ashkar, 1980) and the traditional Intensity-Duration-Frequency (IDF) method,

Hydrol. Earth Syst. Sci. Discuss., doi:10.5194/hess-2016-194, 2016
Manuscript under review for journal Hydrol. Earth Syst. Sci.
Published: 9 May 2016

303 respectively, using the simulated flood and areal rainfall time series for the 50 catchments
304 mentioned in Sect. 3.1. Note that we used the grid rainfall datasets as the input of the GRM
305 model as mentioned in Sect. 2.2 but calculated the areal rainfall time series for each
306 catchment to generate the RIDC. Since the QDF method was initiated in the middle of the
307 1970s and early 1980s (NERC, 1975; Ashkar, 1980), the QDF method has been used in many
308 studies (Balocki and Burges, 1994; Sherwood, 1994; Meunier, 2001; Javelle et al., 2002, 2003;
309 Cunderlik and Ouarda, 2006; Cunderlik and Ouarda, 2007). The QDF method is similar to
310 the IDF. It calculates the average flow by a moving average technique over a given duration
311 and calculates the frequency using the maximum flows extracted from the averaged flows
312 over the given durations (Javelle et al., 2002; Cunderlik and Ouarda, 2006). The frequency
313 analysis is out of range for this study; therefore, we only calculated the maximum flows
314 extracted from the averaged flows over the given durations by the QDF method and
315 generated the FIDC by plotting maximum flows against the durations. The RIDC was
316 generated using the same method of FIDC generation with different inputs for the areal
317 rainfall time series. The units in the FIDC are changed from cubic meter per second (CMS) to
318 mm/h to compare with the units for rainfall intensity in the RIDC. The FIDC and RIDC
319 metrics are useful by coupling with the TC to investigate the relationship between storm
320 types and flood responses as described in Sects. 3.3 and 3.4.

321 3.3 Runoff Coefficient of the Rational Method

322 The runoff coefficient (*C*) of the rational method (Kuichling, 1889) can be calculated by
323 applying the TC to the RIDC and FIDC generated in Sect. 3.2. We have not used the rational
324 method to generate the flow, but have only used the concept of this method to calculate *C*.
325 The TC can be varying with the different storm events but we used the fixed TC values
326 using the Eq. (9), which represent the overall TC value, because we used the TC value as a
327 consistent measure regardless of the different size of the catchments to calculate the factors
328 including *C*. The rational method is as below:

329 $$Q_{peak} = C \times I_{Tc} \times A \quad (7)$$

Hydrol. Earth Syst. Sci. Discuss., doi:10.5194/hess-2016-194, 2016
Manuscript under review for journal Hydrol. Earth Syst. Sci.
Published: 9 May 2016

where Q_{peak} is the peak flow, C is the runoff coefficient, I_{Tc} is the mean rainfall intensity corresponding to the TC (mm/h), and A is the size of the catchment. The value of C is calculated as:

$$C = \frac{q_{peak}}{I_{Tc}} \tag{8}$$

where q_{peak} (mm/h) is calculated as Q_{peak} divided by A and q_{peak} is the peak flow intensity with the changed units. The C represents the effects of the mean rainfall intensity during the TC on the peak flow; therefore, it is an indicator of storm effects on the flood responses of the catchments. This idea is shown in Fig. 2 where Tc represents time of concentration, q_{peak} is the very left value in the FIDC (blue line), and I_{Tc} is the value on the RIDC (red line) corresponding to Tc.

The TC can be used as a consistent measure when extracting the valuable factors from the FIDC and the RIDC for different catchment sizes. We used the TC equation of Kim (1994) as below, which is suitable for the Korean catchment sizes from small to large.

$$Tc = 0.76 \times A^{0.38} \tag{9}$$

Equation (9) has a form similar to those by Boyd (1978), and D'Odorico and Rigon (2003), which demonstrated that the TC equation only with one variable of catchment area is suitable.

3.4 Relationship between the Runoff Coefficient and the Rainfall-Intensity-Ratio for Dependent and Independent Catchments

The value of C was calculated using RIDC, FIDC, and TC as discussed in Sect. 3.3. A factor for the rainfall was needed to analyze the storm effects on C. We calculated the rainfall-intensity-ratio $R1$ below, which is the factor of rainfall corresponding to C.

$$R1 = \frac{P_{peak}}{I_{Tc}} \tag{10}$$

where P_{peak} represents the peak rainfall intensity for one hour duration (the very left value on the RIDC plot in Fig. 2). The variation from the peak rainfall intensity to the mean rainfall

Hydrol. Earth Syst. Sci. Discuss., doi:10.5194/hess-2016-194, 2016
Manuscript under review for journal Hydrol. Earth Syst. Sci.
Published: 9 May 2016

Hydrology and Earth System Sciences
Discussions

intensity during the TC is given as $R1$. It implies that the storm is either an intensive rainfall with a short period or a rainfall with a longer period. If the storm is an intensive rainfall with a short period, then the gradient of the RIDC becomes steeper, and the value of $R1$ increases.

The runoff coefficients of the mean-flood-volume-intensity (MFVI) (C_{vol1} and C_{vol2} in Fig. 2) can be calculated using the RIDC, FIDC and TC as:

$$C_{vol1} = \frac{q_{Tc}}{I_{Tc}} \tag{11}$$

$$C_{vol2} = \frac{q_{Tc2}}{I_{Tc2}} \tag{12}$$

where C_{vol1} and C_{vol2} represent the runoff coefficients of MFVIs corresponding to TC and two times TC, respectively; q_{Tc} and q_{Tc2} are the MFVIs corresponding to TC and two times TC, respectively; and I_{Tc2} is the mean rainfall intensity corresponding to two times TC (mm/h). We calculated the rainfall-intensity-ratios of $R2$ and $R3$ as below (see also Fig. 2) for the additional analyses between the storms and the flood responses.

$$R2 = \frac{I_{Tc2}}{I_{Tc}} \tag{13}$$

$$R3 = \frac{P_{peak}}{I_{Tc2}} \tag{14}$$

The storm effects on the flood responses were analyzed quantitatively by using the factors of the aforementioned runoff coefficients and rainfall-intensity-ratios. We analyzed the storm effects on the flood responses for the two groups, as discussed in Sect. 4.2, of the 15 dependent main-stream catchments that are catchments with increasing size by accumulation from the upper catchments to the lower catchments and of the 35 independent sub-stream catchments. The main-stream catchments are the catchments having outlets on the main stream, the Nakdong River; and the sub-stream catchments are the catchments with outlets on the tributaries of the Nakdong River. For the dependent main-stream catchments, we analyzed the storm effects on flood responses by plotting the runoff coefficients and the rainfall-intensity-ratios versus the catchment size. For the independent

Hydrol. Earth Syst. Sci. Discuss., doi:10.5194/hess-2016-194, 2016
Manuscript under review for journal Hydrol. Earth Syst. Sci.
Published: 9 May 2016

Hydrology and Earth System Sciences
Open Access
Discussions

sub-stream catchments, we analyzed the relationship between storms and floods using the runoff coefficients and the rainfall-intensity-ratios directly without using the catchment size because there was no clear relationship between storms and floods as discussed in Sect. 4.2. The two additional factors of C/C_{vol1} and $R1 \bullet R2$ were used for further analyses as will be described in Sect. 4.5.

4 Results

4.1 Model Performance

Figure 3 shows the NSE, PBIAS, and r_{mod} model performance evaluation statistics for the three catchments (Andongdam, Dosan, and Socheon) over the 20 events. The black dashed lines represent the acceptance boundaries for each statistic as mentioned in Sect. 2.3.

The Andongdam catchment, which is the calibration catchment, has satisfactory NSE, PBIAS, and r_{mod} values for all 20 events. The Dosan and Socheon catchments, which are the validation catchments that are regarded as ungauged catcments, have satisfactory performance statistics except for several events that have inconsistent unsatisfactory results over the three performance statistics. For the Dosan catchment, 2000_Evt1 event has slightly overestimated volume with respect to the PBIAS value. However, the NSE value is very close to the acceptance boundary of 0.5 NSE that could be a satisfactory result and the r_{mod} value is within the acceptance boundary, which represents the satisfactory correlation between simulated and observed flow time series. Therefore, we decided that the simulated flow for the 2000_Evt1 event has an acceptable performance. With the same manner, we screened the unsatisfactory model performances for the events for the Socheon catchment. The event with unsatisfactory results in terms of all three performance evaluation statistics is 2004_Evt1. The main reason for this unsatisfactory result could be the water level measurement error rather than the error in the model structure or input climate data when we consider the acceptable performance evaluation statistic values for the Socheon catchment over the other events and for the other catchments over the 20 events. Therefore,

Hydrol. Earth Syst. Sci. Discuss., doi:10.5194/hess-2016-194, 2016
Manuscript under review for journal Hydrol. Earth Syst. Sci.
Published: 9 May 2016

we accepted this simulation result for the 2004_Evt1 event. The ranges of the three performance evaluation statistics were similar for both the calibration and the validation catchments. It represents that the simulated flows for the validation catchments by the SDE method were generated with the similar error of the simulated flows for the calibration catchment. Hence, the SDE method can generate the acceptable flow time series for the ungauged catchments.

4.2 Relationship between Size of Area and Peak Flow Generated by the SDE Method

We generated the simulated flood time series for the 47 ungauged catchments over the 20 events by the SDE method using the reasonably calibrated parameter values given in Sect. 4.1. The dataset for the total of 50 catchments, including the three gauged catchments, will be used for the analysis in Sects. 4.2 to 4.5.

Figure 4 shows the plots of the maximum rainfall from the areal rainfall time series or the flood values for the 50 catchments versus the size of the area for two of the events as examples. It shows a power law relationship between the maximum rainfall (or flood) values and the catchments when the area is greater than about 100 km^2. This result supports the previous studies that showed that peak flows and catchment sizes have a power law relationship (Gupta and Dawdy, 1995, Goodrich et al, 1997; Gupta and Waymire, 1998; Ogden and Dawdy, 2003). However, there is no clear relationship between the maximum rainfall (or flood) values and the catchments with areas less than about 100 km^2. This result is similar to that found in the work of Cannarozzo et al. (1995), Young et al. (2009), Zoccatelli et al. (2010), and Dhakal et al. (2011). These two types of results demonstrate that the analysis using the dataset generated by the SDE method is as useful as the analysis from previous studies that used observed datasets.

From these results, we hypothesized that analyses are needed by dividing the catchments by size. Sect. 4.4 uses the catchments with an area greater than 100 km^2, which are dependent catchments as mentioned in Sect. 3.4; and Sect. 4.5 uses the independent catchments with an area less than 100 km^2 to analyze the storm effects on floods.

Hydrol. Earth Syst. Sci. Discuss., doi:10.5194/hess-2016-194, 2016
Manuscript under review for journal Hydrol. Earth Syst. Sci.
Published: 9 May 2016

434 4.3 Plot of RIDC and FIDC

435 Figure 5 shows the RIDC and the FIDC determined by the method discussed in Sect. 3.2.
436 The left hand side plot, which is the lowest catchment for the event in 2006, has a relatively
437 lower flood intensity compared to the rainfall intensity. The right hand side plot, which is
438 given for the uppermost catchment for the event in 2009, has a relatively higher flooding
439 intensity as compared to the one in the left hand side plot. The upper catchment, as expected,
440 has the quicker and larger flood response (mm/h) to the rainfall due to a steeper average
441 slope and shallower soil layers. However, the lower catchment with a larger area has a
442 slower and smaller flood response (mm/h) due to more retention, detention, and infiltration
443 of water in the catchment. The water associated with infiltration corresponds to
444 groundwater flow after the event and it is out of the range for this study. Note that the RIDC
445 on the right hand side plot fluctuates. It happens when a storm event has a longer duration
446 of rainfall with varying intensity, such as occurs in the monsoon climate in the Republic of
447 Korea. We found that this type of RIDC occurs frequently in this study.

448 4.4 Relationship between Runoff Ratios and Rainfall-Intensity-Ratios for the Dependent
449 Catchments

450 We plotted the runoff coefficients and the rainfall-intensity-ratios versus the catchment
451 size for the 15 dependent catchments using the methods described in Sects. 3.3 and 3.4 and
452 found that the 20 events can be separated into four types by a combination of the runoff
453 coefficient and the rainfall-intensity-ratio (Fig. 6). For example, Type 1 in Fig. 6 is the case of
454 a decreasing runoff coefficient (C) and an increasing rainfall-intensity-ratio (R) with
455 increasing catchment size (A).

456 Figure 7 shows the plots of C and $R1$ versus the catchment size for events representing
457 each of the four types of events selected from the 20 events.

458 We found, interestingly, that the relationships for C_{vol1}, C_{vol2}, and $R3$ with catchment
459 size are similar to or clearer than the relationships of C and $R1$ with the catchment size for
460 most events when they are classified by type. Figure 8 shows these clearer relationships as

Hydrol. Earth Syst. Sci. Discuss., doi:10.5194/hess-2016-194, 2016
Manuscript under review for journal Hydrol. Earth Syst. Sci.
Published: 9 May 2016

461 compared to the relationships observed in Fig. 7. This result implies that not only the flood
462 peak but also the flood volume should be considered when analyzing the storm effects with
463 different patterns of flood responses.

464 We investigated the hyetographs and hydrographs of the events for the four types and
465 found some relationships for each. Type 1 events have similar rainfall intensity and patterns
466 over the entire catchment. Type 2 events have moving storms in the upper catchment
467 direction. Type 3 events have moving storms in the lower catchment direction. Type 4
468 events have a non-distinctive movement of storms, antecedent rainfall, and strong rainfall
469 intensity with short durations that occur randomly over the catchment.

470 The classification of the four types is reasonable physically. For the case of a Type 1
471 event, when the rainfall falls with similar intensity and pattern over the entire catchment
472 without storm movement (see the similar rainfall intensity of "2007_Evt1 (Type 1)
473 Andongdam" and "2007_Evt1 (Type 1) WP44" in Fig. 9), then the runoff coefficient
474 decreases as the catchment size increases due to increases in the infiltration, the detention,
475 and the retention of water. For the rainfall-intensity-ratio, the values of $R1$ increase as the
476 catchment size increases. This is because the values of P_{peak} are similar, but the larger
477 catchments have longer a TC (see the vertical long dashed line in Fig. 9, TCs in the WP44
478 catchment and in the Andongdam catchment are 6 h and 12 h by rounding up, respectively)
479 causing a smaller value of I_{Tc}, which is used as the denominator in Eq. (10). A Type 1 event
480 will occur more frequently as the size of the entire catchment decreases because there is a
481 greater possibility of a similar intensity and pattern over the entire catchment for the smaller
482 catchments. The other types (Type 2, 3, and 4) have characteristics that are moving storms or
483 spatial variations of the rainfall, such as random local storms.

484 When the storm moves in the upper catchment direction (Type 2), the values of P_{peak}
485 for the upper catchments increase (the value of P_{peak} in "2002_Evt1 (Type 2) WP44" is 2.5
486 times larger than the one in "2002_Evt1 (Type 2) Andongdam" in Fig. 9). Therefore, the
487 values of $R1$ in Eq. (10) for the upper catchments become larger compared to those for the
488 lower catchments. Since the storm moves in the upper catchment direction, the time of the

Hydrol. Earth Syst. Sci. Discuss., doi:10.5194/hess-2016-194, 2016
Manuscript under review for journal Hydrol. Earth Syst. Sci.
Published: 9 May 2016

489 superposition of the flow from the upper catchment to one of the lower catchments is
490 delayed, and accumulated severe floods do not occur for the lower catchments. The runoff
491 coefficients are similar to those in Type 1, but the magnitudes are increased (see the larger
492 gradient for FIDC of "2002_Evt1 (Type 2) Andongdam" compared to the one for "2007_Evt1
493 (Type 1) Andongdam"). The runoff coefficients fluctuate depending on the speed and
494 intensity of the storm. Figure 7 shows this phenomenon well. The values of *C* in the
495 "2002_Evt1 (Type 2)" were more than 0.6, which placed it at a high level compared to the *C*
496 values for the "2007_Evt1 (Type 1)." The values of *C* in "2002_Evt1 (Type 2)" fluctuated with
497 a horizontal trend in the range from 0.6 to 0.65. This horizontal trend became clearer as a
498 Type 2 trend in Fig. 8, which shows that the values of C_{vol1} in "2002_Evt1 (Type 2)" increase
499 as the catchment size decreases.

500 When the storm moves from the upper catchment to the lower catchment (Type 3), the
501 ratio of $P_{peak} : I_{Tc}$ for the upper catchment is larger than that for the lower catchment (see
502 "1998_Evt1 (Type 3) WP44" and "1998_Evt1 (Type 3) Andongdam" in Fig. 9); and, therefore,
503 the values of $R1$ for the upper catchments are larger than those for the lower catchments.
504 The reason is that when the storm moves from the upper catchment to the lower catchment,
505 the areal rainfall intensity for the upper catchment with a smaller area is larger than the one
506 for the lower catchment with a larger area. The RIDC plots the maximum value of the areal
507 rainfall intensity for a given duration by a moving average technique, using the rainfall time
508 series regardless of the exact time of the rainfall. Therefore, the maximum areal rainfall
509 intensity in the RIDC for the upper catchment with a smaller area is larger than that for the
510 lower catchment with a larger area. The increase in the rainfall-intensity-ratios with the
511 decrease in the catchment size implies that movement of storm is not dependent on its
512 direction with regards to the upper or lower catchments. The runoff coefficients increase as
513 the size of the catchments increase because the floods in the lower catchments become
514 extremely large due to storms moving in the direction of the lower catchments concurrent
515 with the arrival of floods flowing down from the upper catchments as mentioned by Roberts
516 and Klingeman (1970).

Hydrol. Earth Syst. Sci. Discuss., doi:10.5194/hess-2016-194, 2016
Manuscript under review for journal Hydrol. Earth Syst. Sci.
Published: 9 May 2016

Hydrology and Earth System Sciences
Open Access
Discussions

When the soil moisture ratio is high due to antecedent rainfall and a storm with non-distinctive movement has strong rainfall intensity with a short duration occurring randomly over the catchment (Type 4), flash floods occur due to the strong rainfall intensity over a short duration. The floods are relatively larger for the lower catchments due to relatively smaller amounts of water infiltrating the ground or being retained (see FIDC for "2003_Ev2 (Type 4) Andongdam" considering I_{Tc} compared to the one for "2003_Ev2 (Type 4) WP44" in Fig. 9). Therefore, the runoff coefficients increase as the catchment size increases. The smaller catchments have larger areal rainfall intensity due to strong local storms (see the RIDC for "2003_Evt2 (Type 4) WP44" compared to the one for "2003_Evt2 (Type 4) Andongdam" in Fig. 9). The gradient of the RIDC is steep even for the lower catchments with large areas due to strong rainfall intensity over short durations; hence, the value of I_{Tc} in Eq. (10) decreases dramatically. Therefore, the value of $R1$ increases as the size of the catchment increases. As shown in Fig. 7, both Type 1 and Type 4 events have increasing values of $R1$ as the catchment size increases, but the magnitudes are different. The values of $R1$ for the "2007_Evt1 (Type 1)" are in the range from 1.4 to 1.9, but the ones for the "2003_Evt2 (Type 4)" ranged from 2.5 to 4 due to the characteristic of significant decrement.

The analyses described above show that the characteristics of the storm are the main drivers for the characteristics of the flood responses. Therefore, the analytical method in this section is useful for the investigation of the relationship between storm patterns and flood responses, quantitatively. We investigated the frequency of each type of event for the 20 events, showing that 13 events are Type 1 (65%), four events are Type 2 (20%), two events are Type 3 (10%), and one event is Type 4 (5%). These frequency results cannot be generalized due to the small number of events, but it shows definite trends. Other researchers can use their own datasets with a greater number of events to generalize the frequency of these types.

4.5 Relationship between Runoff Ratios and Rainfall-Intensity-Ratios for the Independent Catchments

Hydrol. Earth Syst. Sci. Discuss., doi:10.5194/hess-2016-194, 2016
Manuscript under review for journal Hydrol. Earth Syst. Sci.
Published: 9 May 2016

Hydrology and Earth System Sciences
Open Access
Discussions

In this section, we investigate the relationship between the runoff coefficients and the rainfall-intensity-ratios for the 35 independent sub-stream catchments with areas less than 100 km², as discussed in Sect. 4.2. The catchment WP17 (231.7 km²) is slightly large, but we surmise that the effect of this catchment is minor for the analysis. We cannot find the clear relationship between the runoff coefficients and the rainfall-intensity-ratios for the independent catchments over the 20 events due to a random distribution. The C values for the independent catchments with I_{Tc} values less than 15 mm varied randomly (not shown here). The reason could be the large initial loss by infiltration due to very low initial soil moisture contents or the relatively large antecedent flow, which affect the flood responses. It implies that different regions have different rainfall intensity during the same event, and the independent catchments with low rainfall intensity have different flood responses. Therefore, we analyzed the relationship between the runoff coefficients and the rainfall-intensity-ratios for the independent catchments with I_{Tc} values greater than 15 mm. However, four events ("2000_Evt1", "2003_Evt1", "2006_Evt3", "2007_Evt1") do not have independent catchments with more than 15 mm of I_{Tc}, so we used only 16 events for the analysis.

As a result, the relationship between C and $R1$ is not always clear even for the independent catchments with more than 15 mm of I_{Tc} (Fig. 10). Therefore, we used the additional runoff coefficient (C/C_{vol1}) and the rainfall-intensity-ratio ($R1 \bullet R2$) as given below to investigate the relationship.

$$C/C_{vol1} = \frac{q_{peak}}{q_{Tc}} \tag{15}$$

The C/C_{vol1} represents the storm effect on the variation of the flood volume. The value of C/C_{vol1} increases as the value of q_{Tc} decreases; therefore, the value of C/C_{vol1} becomes significantly larger as the flood volume becomes significantly smaller as indicated when the hydrograph plunged down from the q_{peak}.

$$R1 \bullet R2 = \frac{P_{peak} \times I_{Tc2}}{\left(I_{Tc}\right)^2} \tag{16}$$

Hydrol. Earth Syst. Sci. Discuss., doi:10.5194/hess-2016-194, 2016
Manuscript under review for journal Hydrol. Earth Syst. Sci.
Published: 9 May 2016

571 The $R1 \bullet R2$ represents the variation of the rainfall intensity by the value of I_{Tc}
572 between P_{peak} and I_{Tc2}. The value of $R1 \bullet R2$ increases as the value of I_{Tc} decreases;
573 therefore, a significantly large value of $R1 \bullet R2$ represents a significant reduction of rainfall
574 intensity from P_{peak} to I_{Tc}.

575 Table 2 shows the correlation coefficients for the relationships between C and $R1$,
576 between C and $R1 \bullet R2$, between C/C_{vol1} and $R1$, and between C/C_{vol1} and $R1 \bullet R2$. The
577 "Type" represents the four types of events as described in Sect. 4.4. The bold number
578 represents the highest correlation coefficient for each event, and the underlined number
579 represents the second highest correlation coefficient for each event. The notation, "No. 1st
580 corr.," at the bottom of the table represents the number of events with the highest correlation
581 coefficient for each combination of runoff coefficient and rainfall-intensity-ratio. The
582 notation, "No. 2nd corr.," is the number of events with the second highest correlation
583 coefficient; and the notation, "Total," is the summation of "No. 1st corr." and "No. 2nd corr."
584 for each combination. We also investigated the correlations using the data of $R1$ and
585 $R1 \bullet R2$ transformed by log, square root, and exponential transformations (not shown here);
586 however, the results are similar to the one with non-transformed data. Therefore, we show
587 the results with non-transformed data only.

588 As shown in Table 2, the combination having the highest correlation coefficient is
589 different for each event. The combinations of C with $R1$ and C/C_{vol1} with $R1$ had the
590 highest frequency in terms of having the highest correlation coefficient ("No. 1st corr."), and
591 the "Total" also showed the similar result. The $R1$ factor is the major factor that affects the
592 flood peak (C) and the flood volume (C/C_{vol1}). As shown by "Type" in Table 2, the
593 correlations between the runoff coefficients and the rainfall-intensity-ratios for the
594 independent catchments have no relationship with the type of events (see the variation of
595 highest correlation coefficients over the combinations in the Type 1 events).
596

597 **5 Discussion and Conclusions**

Hydrol. Earth Syst. Sci. Discuss., doi:10.5194/hess-2016-194, 2016
Manuscript under review for journal Hydrol. Earth Syst. Sci.
Published: 9 May 2016

598 This study analyzed the relationship between natural storm patterns and flood
599 responses, quantitatively, for various catchment sizes by coupling the TC with the FIDC and
600 the RIDC. We demonstrated the usefulness of the time of concentration for both small and
601 large catchments. The time of concentration should be calculated using the time of
602 concentration function suitable for the study catchments as shown in this study. We
603 recommend that other researchers use the time of concentration function suitable for their
604 study area.

605 The SDE method suggested in this study is a relatively easy method to use with good
606 applicability for generating the flood time series for the ungauged catchments. This reduced
607 the difficulties of not enough flow data for the hydrological analysis. The data simulated by
608 this method could have errors, but it gives guidance in analyzing and understanding the
609 general hydrological responses as shown in this study. The analysis of hydrological
610 responses using the simulated data for the ungauged catchments by the SDE method has the
611 weakness of relying on the rainfall-runoff model structure. Therefore, an uncertainty
612 analysis (e.g. Shin et al,, 2013, 2015) for the GRM model needs to be conducted, but it is out
613 of the scope of this study. However, the analytical methods used in this study can use any
614 physically based distributed model with less structural uncertainty.

615 To summarize, this study investigated the storm pattern effects on the flood responses
616 for various catchment sizes using a distributed rainfall-runoff model. We calibrated the
617 parameters of the GRM model for 20 events that had good quality data and calculated the
618 NSE values for the simulated hydrographs. The result showed that 90% of the simulated
619 hydrographs have NSE values greater than 0.5. Therefore, the GRM model was applicable
620 for the study catchments. The hydrographs for the 47 ungauged catchments were generated
621 by the SDE method for the 20 events; and the peak values extracted from the areal rainfall
622 and flood time series for the total 50 catchments, which included the three gauged
623 catchments, were plotted versus the catchment size. The result showed that there was a
624 power law relationship between the peak values and the catchment size for areas greater
625 than about 100 km^2, whereas, there was no clear relationship due to a large dispersion of

Hydrol. Earth Syst. Sci. Discuss., doi:10.5194/hess-2016-194, 2016
Manuscript under review for journal Hydrol. Earth Syst. Sci.
Published: 9 May 2016

626 peak values for the catchments with areas less than about 100 km^2. We generated the FIDC
627 and the RIDC for the 50 catchments and calculated the runoff coefficients and the
628 rainfall-intensity-ratios by coupling the time of concentration with the FIDC and the RIDC
629 and then analyzed the relationship between the runoff coefficients and the
630 rainfall-intensity-ratios for the dependent (greater than about 100 km^2) and independent
631 (less than about 100 km^2) catchments. As a result, the 20 events were separated into four
632 physically reasonable event types by a combination of storm patterns and flood responses
633 for the dependent catchments. It showed that the relationship between storm patterns and
634 flood responses for any event can be analyzed quantitatively by plotting the runoff
635 coefficients or the rainfall-intensity-ratios versus the size of the dependent catchments.
636 Lastly, there are correlations between $R1$ and C and between $R1$ and C/C_{vol1} for the
637 independent catchments with I_{Tc} values more than 15 mm, but these correlations have no
638 relationship with the four types of events from the dependent catchments.
639
640

Hydrol. Earth Syst. Sci. Discuss., doi:10.5194/hess-2016-194, 2016
Manuscript under review for journal Hydrol. Earth Syst. Sci.
Published: 9 May 2016

Hydrology and Earth System Sciences
Discussions

Appendix A: Tables for descriptions of catchments characteristics and selected events

Table A1. Size of area, average slope, channel length, and the class of catchment for the 50 catchments.[a]

Name	Area(km²)	Ave. slope	Ch. L(km)	Class	Name	Area(km²)	Ave. slope	Ch. L(km)	Class
Andongdam	1584.2	0.21	147.2	Main	WP26	751.4	0.24	82.5	Main
WP2	14.7	0.19	5.6	Sub	WP27	39.1	0.24	10.6	Sub
WP3	1459.7	0.21	132.4	Main	WP28	28.4	0.27	11.1	Sub
WP4	51.6	0.10	12.6	Sub	Socheon	645.0	0.25	62.5	Main
WP5	13.8	0.13	5.3	Sub	WP30	104.5	0.28	20.8	Sub
WP6	1327.7	0.23	119.6	Main	WP31	32.7	0.30	7.4	Sub
WP7	89.6	0.20	19.9	Sub	WP32	540.0	0.24	61.7	Main
WP8	81.2	0.21	16.4	Sub	WP33	88.5	0.21	23.3	Sub
WP9	17.6	0.20	5.5	Sub	WP34	37.3	0.21	10.1	Sub
WP10	1235.9	0.23	118.4	Main	WP35	402.1	0.25	49.9	Main
WP11	1221.5	0.23	114.0	Main	WP36	33.9	0.22	9.3	Sub
WP12	36.6	0.14	12.6	Sub	WP37	13.0	0.24	4.6	Sub
Dosan	1157.4	0.23	101.6	Main	WP38	60.5	0.24	14.2	Sub
WP14	8.9	0.23	5.8	Sub	WP39	23.2	0.24	7.4	Sub
WP15	1142.6	0.23	99.5	Main	WP40	251.2	0.25	29.2	Main
WP16	11.2	0.25	5.6	Sub	WP41	49.2	0.26	12.8	Sub
WP17	231.7	0.19	33.1	Sub	WP42	22.2	0.28	9.0	Sub
WP18	34.0	0.10	6.5	Sub	WP43	14.2	0.22	4.2	Sub
WP19	5.6	0.13	4.3	Sub	WP44	189.9	0.25	25.2	Main
WP20	28.6	0.29	7.5	Sub	WP45	58.6	0.24	15.1	Sub
WP21	47.0	0.24	10.8	Sub	WP46	131.2	0.25	24.6	Sub
WP22	850.0	0.24	89.5	Main	WP47	41.6	0.27	10.9	Sub
WP23	838.8	0.24	83.1	Main	WP48	32.6	0.28	7.7	Sub
WP24	86.4	0.18	20.3	Sub	WP49	53.6	0.23	12.5	Sub
WP25	39.2	0.18	10.2	Sub	WP50	19.6	0.25	7.0	Sub

[a] The Main in the Class column represents the main-stream catchments that are the catchments having outlets on the main stream, the Nakdong River; and the Sub in the Class column represents the sub-stream catchments that are the catchments with outlets on the tributaries of the Nakdong River.

Hydrol. Earth Syst. Sci. Discuss., doi:10.5194/hess-2016-194, 2016
Manuscript under review for journal Hydrol. Earth Syst. Sci.
Published: 9 May 2016

Hydrology and Earth System Sciences
Open Access
Discussions

649 **Table A2.** Period of the 20 events.

Event	Period	Event	Period
1998_Evt1	1998081419-1998081723	2004_Evt1	2004061904-2004062303
1999_Evt1	1999080213-1999080504	2004_Evt2	2004071509-2004071902
1999_Evt2	1999091920-1999092201	2004_Evt3	2004081719-2004082022
1999_Evt3	1999092304-1999092519	2006_Evt1	2006071007-2006071208
2000_Evt1	2000091301-2000091518	2006_Evt2	2006071514-2006071710
2000_Evt2	2000091604-2000091804	2006_Evt3	2006072804-2006073101
2002_Evt1	2002080520-2002080916	2007_Evt1	2007090102-2007090317
2002_Evt2	2002083023-2002090204	2008_Evt1	2008072419-2008072703
2003_Evt1	2003062709-2003062918	2009_Evt1	2009071121-2009071408
2003_Evt2	2003091124-2003091501	2009_Evt2	2009071415-2009071622

650

Hydrol. Earth Syst. Sci. Discuss., doi:10.5194/hess-2016-194, 2016
Manuscript under review for journal Hydrol. Earth Syst. Sci.
Published: 9 May 2016

Acknowledgements

This research was supported by a grant (11-TI-C06) from the Advanced Water Management Research Program funded by the Ministry of Land, Infrastructure and Transport of the Korean government. We gratefully acknowledge Yun Seok Choi for valuable discussions regarding the study.

Hydrol. Earth Syst. Sci. Discuss., doi:10.5194/hess-2016-194, 2016
Manuscript under review for journal Hydrol. Earth Syst. Sci.
Published: 9 May 2016

References

Alexander, G. N.: Effect of catchment area on flood magnitude, J. Hydrol., 16(3), 225-240, 1972.

Anquetin, S., Braud, I., Vannier, O., Viallet, P., Boudevillain, B., Creutin, J. D., and Manus, C.: Sensitivity of the hydrological response to the variability of rainfall fields and soils for the Gard 2002 flash-flood event, J. Hydrol., 394(1), 134-147, 2010.

Arnaud, P., Bouvier, C., Cisneros, L., and Dominguez, R.: Influence of rainfall spatial variability on flood prediction, J. Hydrol., 260(1), 216-230, 2002.

ASCE: Criteria for evaluation of watershed models, J. Irri. Drain. Eng., 119(3), 429-442, 1993.

Ashkar, F.: Partial duration series models for flood analysis, Ph.D. Thesis, École Polytechnique de Montréal, Montréal, Canada, 1980.

Balocki, J. B., and Burges, S. J.: Relationships between n-day flood volumes for infrequent large floods, J. Water Resour. Plann. Manage., 120(6), 794-818, 1994.

Bathurst, J. C.: Sensitivity analysis of the Systeme Hydrologique Europeen for an upland catchment, J. Hydrol., 87(1), 103-123, 1986.

Bell, V. A., and Moore, R. J.: The sensitivity of catchment runoff models to rainfall data at different spatial scales, Hydrol. Earth Syst. Sci. Discussions, 4(4), 653-667, 2000.

Beven, K.: Kinematic subsurface stormflow, Water Resour. Res., 17(5), 1419-1424, 1981.

Bhaskar, N. R., Parida, B. P., and Nayak, A. K.: Flood estimation for ungauged catchments using the GIUH, J. Water Resour. Plann. Manage., 123(4), 228-238, 1997.

Boyd, M. J.: A storage-routing model relating drainage basin hydrology and geomorphology, Water Resour. Res., 14(5), 921-928, 1978.

Bronstert, A., and Bárdossy, A.: Uncertainty of runoff modelling at the hillslope scale due to temporal variations of rainfall intensity, Phys. Chem. Earth, Parts A/B/C 28(6), 283-288, 2003.

Cannarozzo, M., D'asaro, F., and Ferro, V.: Regional rainfall and flood frequency analysis for Sicily using the two component extreme value distribution, Hydrol. Sci. J., 40(1), 19-42, 1995.

Hydrol. Earth Syst. Sci. Discuss., doi:10.5194/hess-2016-194, 2016
Manuscript under review for journal Hydrol. Earth Syst. Sci.
Published: 9 May 2016

686 Chaplot, V., Saleh, A., and Jaynes, D. B.: Effect of the accuracy of spatial rainfall information
687 on the modeling of water, sediment, and NO 3–N loads at the watershed level, J. Hydrol.,
688 312(1), 223-234, 2005.
689 Choi, Y. S., Choi, C. K., Kim, H. S., Kim, K. T., and Kim, S.: Multi-site calibration using a
690 grid-based event rainfall–runoff model: a case study of the upstream areas of the
691 Nakdong River basin in Korea, Hydrol. Process., 29(9), 2089-2099, 2015.
692 Chow, V. T., Maidment, D. R., and Mays, L. W.: Applied hydrology, McGraw-Hill, 1988.
693 Cunderlik, J. M., and Ouarda, T. B.: Regional flood-duration–frequency modeling in the
694 changing environment, J. Hydrol., 318(1), 276-291, 2006.
695 Cunderlik, J. M., and Ouarda, T. B.: Regional flood–rainfall duration-frequency modeling at
696 small ungaged sites, J. Hydrol., 345(1), 61-69, 2007.
697 Dawson, C. W., Abrahart, R. J., Shamseldin, A. Y., and Wilby, R. L.: Flood estimation at
698 ungauged sites using artificial neural networks, J. Hydrol., 319(1), 391-409, 2006.
699 Dhakal, N., Fang, X., Cleveland, T. G., Thompson, D. B., Asquith, W. H., and Marzen, L. J.:
700 Estimation of volumetric runoff coefficients for Texas watersheds using land-use and
701 rainfall-runoff data, J. Irrig. Drain. Eng., 138(1), 43-54, 2011.
702 D'Odorico, P., and Rigon, R.: Hillslope and channel contributions to the hydrologic
703 response, Water Resour. Res., 39(5), 1113, 2003.
704 Duncan, M. R., Austin, B., Fabry, F., and Austin, G. L.: The effect of gauge sampling density
705 on the accuracy of streamflow prediction for rural catchments, J. Hydrol., 142(1), 445-476,
706 1993.
707 Faurès, J. M., Goodrich, D. C., Woolhiser, D. A., and Sorooshian, S.: Impact of small-scale
708 spatial rainfall variability on runoff modeling, J. Hydrol., 173(1), 309-326, 1995.
709 Freeze, R. A., and Cherry, J.A.: Groundwater, Prentice Hall Inc., New Jersey, 15-236, 1979.
710 Goodrich, D. C., Lane, L. J., Shillito, R. M., Miller, S. N., Syed, K. H., and Woolhiser, D. A.:
711 Linearity of basin response as a function of scale in a semiarid watershed, Water Resour.
712 Res., 33(12), 2951-2965, 1997.

Hydrol. Earth Syst. Sci. Discuss., doi:10.5194/hess-2016-194, 2016
Manuscript under review for journal Hydrol. Earth Syst. Sci.
Published: 9 May 2016

713 Goswami, M., O'Connor, K. M., and Bhattarai, K. P.: Development of regionalisation
714 procedures using a multi-model approach for flow simulation in an ungauged catchment,
715 J. Hydrol., 333(2), 517-531, 2007.
716 Gupta, V. K., and Dawdy, D. R.: Physical interpretations of regional variations in the scaling
717 exponents of flood quantiles, Hydrol. Process., 9(3-4), 347-361, 1995.
718 Gupta, V. K., and Waymire, E.: Spatial variability and scale invariance in hydrologic
719 regionalization, In Scale dependence and scale invariance in hydrology, Sposito G (eds).,
720 Cambridge University Press, 88-135, 1998.
721 Gupta, H. V., Sorooshian, S., and Yapo, P. O.: Status of automatic calibration for hydrologic
722 models: Comparison with multilevel expert calibration, J. Hydrol. Eng., 4(2), 135-143,
723 1999.
724 Huang, J. C., Kao, S. J., Lin, C. Y., Chang, P. L., Lee, T. Y., and Li, M. H.: Effect of
725 subsampling tropical cyclone rainfall on flood hydrograph response in a subtropical
726 mountainous catchment, J. Hydrol., 409(1), 248-261, 2011.
727 Javelle, P., Ouarda, T. B., and Bobée, B.: Spring flood analysis using the flood-duration–
728 frequency approach: application to the provinces of Quebec and Ontario, Canada, Hydrol.
729 Process., 17(18), 3717-3736, 2003.
730 Javelle, P., Ouarda, T. B., Lang, M., Bobée, B., Galéa, G., and Grésillon, J. M.: Development of
731 regional flood-duration–frequency curves based on the index-flood method, J. Hydrol.,
732 258(1), 249-259, 2002.
733 Kim, N. W.: A comparative study on the evaluation of rainstorm runoff characteristics at
734 ungauged location – on the rational method, Research report Contribution No. 94-WR-112,
735 280pp., Korea Institute of Construction Technology, Republic of Korea, (In Korean), 1994.
736 Klemeš, V.: Operational testing of hydrological simulation models, Hydrol. Sci. J., 31(1),
737 13-24, 1986.
738 Krajewski, W. F., Lakshmi, V., Georgakakos, K. P., and Jain, S. C.: A Monte Carlo study of
739 rainfall sampling effect on a distributed catchment model, Water Resour. Res., 27(1),
740 119-128, 1991.

Hydrol. Earth Syst. Sci. Discuss., doi:10.5194/hess-2016-194, 2016
Manuscript under review for journal Hydrol. Earth Syst. Sci.
Published: 9 May 2016

741 Krause, P., Boyle, D. P., and Bäse, F.: Comparison of different efficiency criteria for
742 hydrological model assessment, Adv. Geosci., 5, 89-97, 2005.
743 Kuczera, G., and Williams, B. J.: Effect of rainfall errors on accuracy of design flood
744 estimates, Water Resour. Res., 28(4), 1145-1153, 1992.
745 Kuichling, E.: The relation between the rainfall and the discharge of sewers in populous
746 districts, T. Am. Soc. Civ. Eng., 20(1), 1-56, 1889.
747 Legates, D. R., and McCabe, G. J.: Evaluating the use of "goodness-of-fit" measures in
748 hydrologic and hydroclimatic model validation, Water Resour. Res., 35(1), 233-241, 1999.
749 Lobligeois, F., Andreassian, V., Perrin, C., Tabary, P., and Loumagne, C.: When does higher
750 spatial resolution rainfall information improve streamflow simulation? An evaluation
751 using 3620 flood events, Hydrol. Earth Syst. Sci., 18(2), 575-594, 2014.
752 Mapiam, P. P., and Sriwongsitanon, N.: Estimation of the URBS model parameters for flood
753 estimation of ungauged catchments in the upper Ping river basin, Thailand, ScienceAsia,
754 35(2009), 49-56, 2009.
755 McCuen, R. H., and Snyder, W. M.: A proposed index for comparing hydrographs, Water
756 Resour. Res., 11(6), 1021-1024, 1975.
757 Meunier, M.: Regional flow–duration–frequency model for the tropical island of Martinique,
758 J. Hydrol., 247(1), 31-53, 2001.
759 Michaud, J. D., and Sorooshian, S.: Effect of rainfall-sampling errors on simulations of desert
760 flash floods, Water Resour. Res., 30(10), 2765-2775, 1994.
761 Moreno, H. A., Vivoni, E. R., and Gochis, D. J.: Utility of quantitative precipitation estimates
762 for high resolution hydrologic forecasts in mountain watersheds of the Colorado Front
763 Range, J. Hydrol., 438, 66-83, 2012.
764 Moriasi, D. N., Arnold, J. G., Van Liew, M. W., Bingner, R. L., Hrmel, R. D., and Veith, T. L.:
765 Model evaluation guidelines for systematic quantification of accuracy in watershed
766 simulations, T. ASABE, 50(3), 885-900, 2007.
767 Nash, J. E., and Sutcliffe, J. V.: River flow forecasting through conceptual models part I - A
768 discussion of principles, J. Hydrol., 10(3), 282-290, 1970.

Hydrol. Earth Syst. Sci. Discuss., doi:10.5194/hess-2016-194, 2016
Manuscript under review for journal Hydrol. Earth Syst. Sci.
Published: 9 May 2016

769 NERC: Estimation of flood volumes over different durations, Flood Studies Report, Vol. 1,
770 Chapter 5, 243–264, 1975.
771 Nicótina, L., Alessi Celegon, E., Rinaldo, A., and Marani, M.: On the impact of rainfall
772 patterns on the hydrologic response, Water Resour. Res., 44(12), W12401, 2008.
773 Obled, C., Wendling, J., and Beven, K.: The sensitivity of hydrological models to spatial
774 rainfall patterns: an evaluation using observed data, J. Hydrol., 159(1), 305-333, 1994.
775 Ogden, F. L., and Dawdy, D. R.: Peak discharge scaling in small Hortonian watershed, J.
776 Hydrol. Eng., 8(2), 64-73, 2003.
777 Ogden, F. L., and Julien, P. Y.: Runoff sensitivity to temporal and spatial rainfall variability
778 at runoff plane and small basin scales, Water Resour. Res., 29(8), 2589-2597, 1993.
779 Oudin, L., Kay, A., Andréassian, V., and Perrin, C.: Are seemingly physically similar
780 catchments truly hydrologically similar?, Water Resour. Res., 46(11), W11558, 2010.
781 Parajka, J., Blöschl, G., and Merz, R.: Regional calibration of catchment models: Potential for
782 ungauged catchments, Water Resour. Res., 43(6), W06406, 2007.
783 Paschalis, A., Fatichi, S., Molnar, P., Rimkus, S., and Burlando, P.: On the effects of small
784 scale space–time variability of rainfall on basin flood response, J. Hydrol., 514, 313-327,
785 2014.
786 Reed, S., Schaake, J., and Zhang, Z.: A distributed hydrologic model and threshold
787 frequency-based method for flash flood forecasting at ungauged locations, J. Hydrol.,
788 337(3), 402-420, 2007.
789 Roberts, M. C., and Klingeman, P. C.: The influence of landform and precipitation
790 parameters on flood hydrographs, J. Hydrol., 11(4), 393-411, 1970.
791 Sargent, D. M.: Investigation into the Effects of Storm Movement on the Design of Urban
792 Drainage Systems: Part 1, Public Health Eng., 9(4), 201-207, 1981.
793 Sargent, D. M.: An investigation into the effects of storm movement on the design of urban
794 drainage systems: Part 2. Probability analysis, Public Health Eng., 10(2), 111-117, 1982.

Hydrol. Earth Syst. Sci. Discuss., doi:10.5194/hess-2016-194, 2016
Manuscript under review for journal Hydrol. Earth Syst. Sci.
Published: 9 May 2016

795 Saulnier, G. M., and Le Lay, M.: Sensitivity of flash-flood simulations on the volume, the
796 intensity, and the localization of rainfall in the Cévennes-Vivarais region (France), Water
797 Resour. Res., 45(10), W10425, 2009.
798 Schuurmans, J. M., and Bierkens, M. F. P.: Effect of spatial distribution of daily rainfall on
799 interior catchment response of a distributed hydrological model, Hydrol. Earth Syst. Sci.
800 Discussions, 11(2), 677-693, 2007.
801 Segond, M. L., Wheater, H. S., and Onof, C.: The significance of spatial rainfall
802 representation for flood runoff estimation: A numerical evaluation based on the Lee
803 catchment, UK, J. Hydrol., 347(1), 116-131, 2007.
804 Shin, M. J., Guillaume, J. H., Croke, B. F., and Jakeman, A. J.: Addressing ten questions
805 about conceptual rainfall–runoff models with global sensitivity analyses in R, J. Hydrol.,
806 503, 135-152, 2013.
807 Shin, M. J., Guillaume, J. H., Croke, B. F., and Jakeman, A. J.: A review of foundational
808 methods for checking the structural identifiability of models: Results for rainfall-runoff, J.
809 Hydrol., 520, 1-16, 2015.
810 Shah, S. M. S., O'Connell, P. E., and Hosking, J. R. M.: Modelling the effects of spatial
811 variability in rainfall on catchment response. 2. Experiments with distributed and lumped
812 models, J. Hydrol., 175(1), 89-111, 1996.
813 Sherwood, J. M.: Estimation of volume-duration-frequency relations of ungaged small
814 urban streams in ohio1, JAWRA J. Am. Water Resour. Assoc., 30(2), 261-269, 1994.
815 Singh, V. P.: Effect of spatial and temporal variability in rainfall and watershed
816 characteristics on stream flow hydrograph, Hydrol. Process., 11(12), 1649-1669, 1997.
817 Smith, M. B., Koren, V. I., Zhang, Z., Reed, S. M., Pan, J. J., and Moreda, F.: Runoff response
818 to spatial variability in precipitation: an analysis of observed data, J. Hydrol., 298(1),
819 267-286, 2004.
820 Smith, M. B., Koren, V., Zhang, Z., Zhang, Y., Reed, S. M., Cui, Z., Moreda, F., Cosgrove, B.
821 A., Mizukami, N., and Anderson, E. A.: Results of the DMIP 2 Oklahoma experiments, J.
822 Hydrol., 418-419, 17-48, 2012.

823 Smith, M. B., Seo, D. J., Koren, V. I., Reed, S. M., Zhang, Z., Duan, Q., ..., and Cong, S.: The
824 distributed model intercomparison project (DMIP): motivation and experiment design, J.
825 Hydrol., 298(1), 4-26, 2004.
826 Syed, K. H., Goodrich, D. C., Myers, D. E., and Sorooshian, S.: Spatial characteristics of
827 thunderstorm rainfall fields and their relation to runoff, J. Hydrol., 271(1), 1-21, 2003.
828 Takeuchi, K., Ao, T., and Ishidaira, H.: Introduction of block-wise use of TOPMODEL and
829 Muskingum-Cunge method for the hydroenvironmental simulation of a large ungauged
830 basin, Hydrol. Sci. J., 44(4), 633-646, 1999.
831 Tewolde, M. H., and Smithers, J. C.: Flood routing in ungauged catchments using
832 Muskingum methods, Water SA, 32(3), 379-388, 2007.
833 Vischel, T., and Lebel, T.: Assessing the water balance in the Sahel: Impact of small scale
834 rainfall variability on runoff. Part 2: Idealized modeling of runoff sensitivity, J. Hydrol.,
835 333(2), 340-355, 2007.
836 Vischel, T., Lebel, T., Massuel, S., and Cappelaere, B.: Conditional simulation schemes of
837 rain fields and their application to rainfall–runoff modeling studies in the Sahel, J. Hydrol.,
838 375(1), 273-286, 2009.
839 Viviroli, D., Mittelbach, H., Gurtz, J., and Weingartner, R.: Continuous simulation for flood
840 estimation in ungauged mesoscale catchments of Switzerland–Part II: Parameter
841 regionalisation and flood estimation results, J. Hydrol., 377(1), 208-225, 2009.
842 Wood, E. F., Sivapalan, M., Beven, K., and Band, L.: Effects of spatial variability and scale
843 with implications to hydrologic modeling, J. Hydrol., 102(1), 29-47, 1988.
844 Woolhiser, D. A., and Goodrich, D. C.: Effect of storm rainfall intensity patterns on surface
845 runoff, J. Hydrol., 102(1), 335-354, 1988.
846 Xu, H., Xu, C. Y., Chen, H., Zhang, Z., and Li, L.: Assessing the influence of rain gauge
847 density and distribution on hydrological model performance in a humid region of China, J.
848 Hydrol., 505, 1-12, 2013.
849 Young, C. B., McEnroe, B. M., and Rome, A. C.: Empirical determination of rational method
850 runoff coefficients, J. Hydrol. Eng., 14(12), 1283-1289, 2009.

Hydrol. Earth Syst. Sci. Discuss., doi:10.5194/hess-2016-194, 2016
Manuscript under review for journal Hydrol. Earth Syst. Sci.
Published: 9 May 2016

851 Zhao, F., Zhang, L., Chiew, F. H., Vaze, J., and Cheng, L.: The effect of spatial rainfall
852 variability on water balance modelling for south-eastern Australian catchments, J. Hydrol.,
853 493, 16-29, 2013.
854 Zoccatelli, D., Borga, M., Zanon, F., Antonescu, B., and Stancalie, G.: Which rainfall spatial
855 information for flash flood response modelling? A numerical investigation based on data
856 from the Carpathian range, Romania, J. Hydrol., 394(1), 148-161, 2010.
857

Hydrol. Earth Syst. Sci. Discuss., doi:10.5194/hess-2016-194, 2016
Manuscript under review for journal Hydrol. Earth Syst. Sci.
Published: 9 May 2016

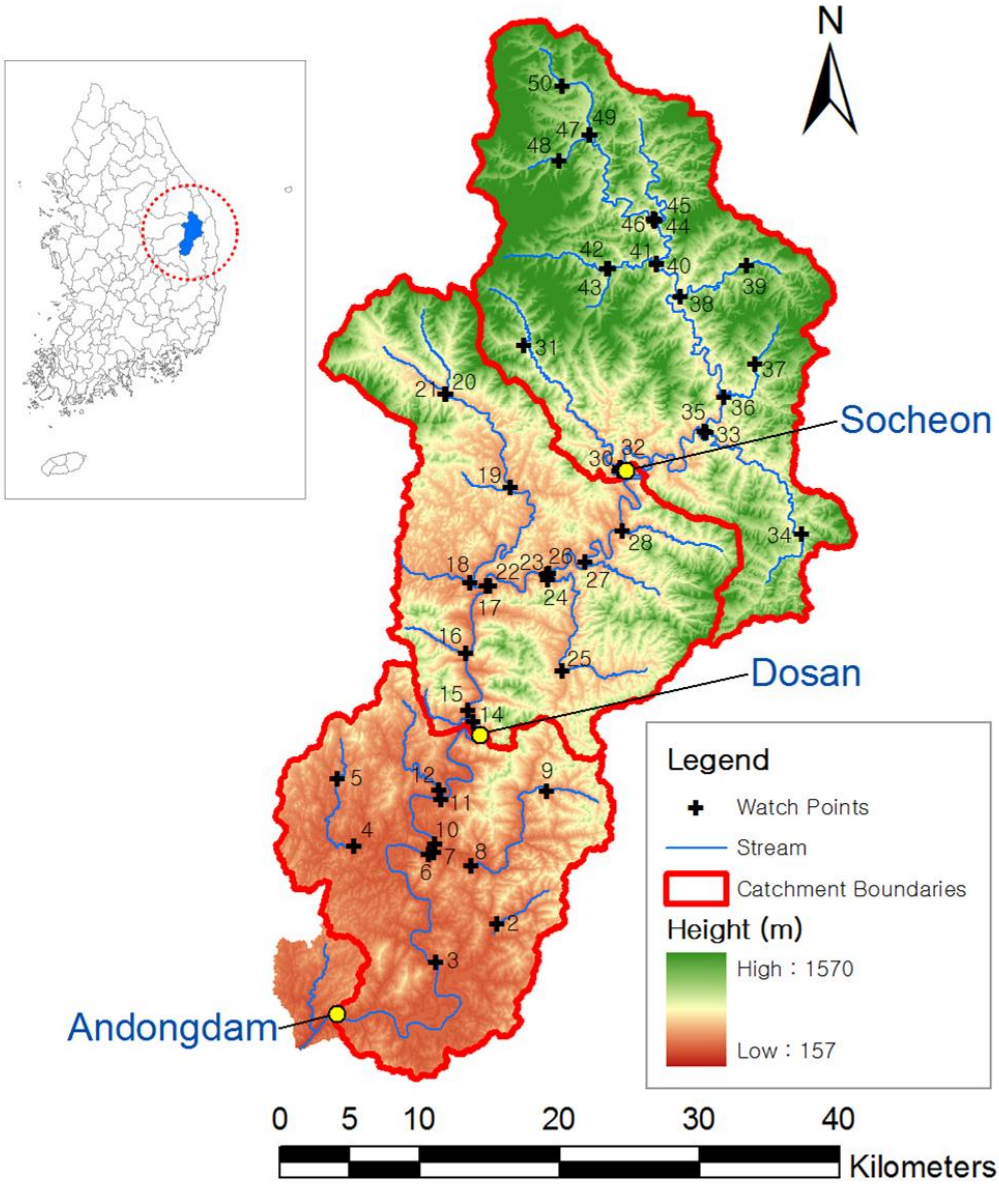

858

859 **Figure 1.** Location and topography of the Andongdam catchment in the Republic of

860 Korea. The yellow points represent the water level gauging stations.

861

862

Hydrol. Earth Syst. Sci. Discuss., doi:10.5194/hess-2016-194, 2016
Manuscript under review for journal Hydrol. Earth Syst. Sci.
Published: 9 May 2016

Hydrology and Earth System Sciences
Discussions

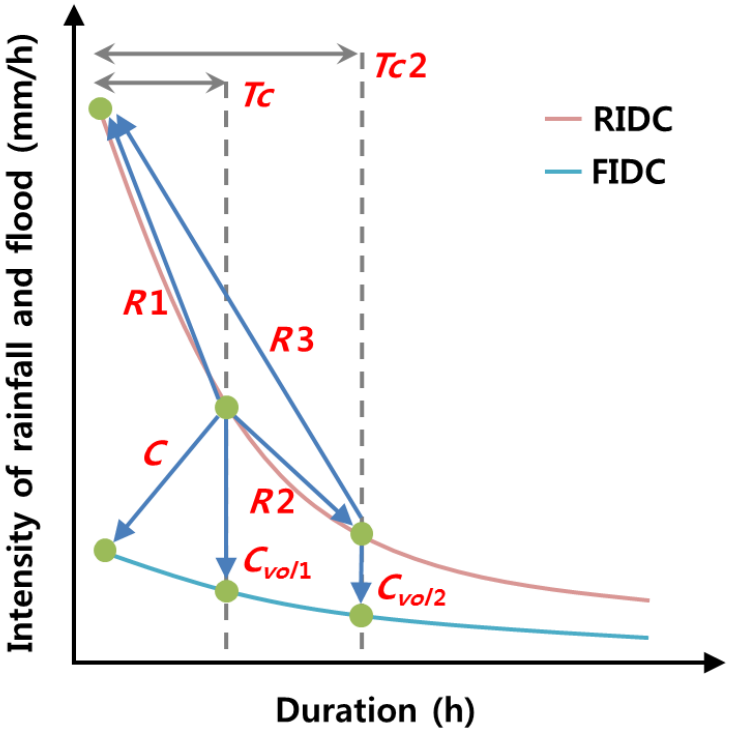

Figure 2. Schematic plot for calculation of runoff coefficient and rainfall-intensity-ratio. *Tc* represents time of concentration (TC) that is a duration (h), *Tc*2 is two times TC, *C* is runoff coefficient, C_{vol1} is the runoff coefficient of mean-flood-volume-intensity (MFVI) at TC, C_{vol2} is the runoff coefficient of MFVI at two times TC, $R1$ is the ratio between the rainfall peak and the mean rainfall intensity at TC (I_{Tc}), $R2$ is the ratio between I_{Tc} and the mean rainfall intensity at two times TC (I_{Tc2}), and $R3$ is the ratio between the rainfall peak and I_{Tc2}.

Hydrol. Earth Syst. Sci. Discuss., doi:10.5194/hess-2016-194, 2016
Manuscript under review for journal Hydrol. Earth Syst. Sci.
Published: 9 May 2016

Hydrology and Earth System Sciences
Discussions

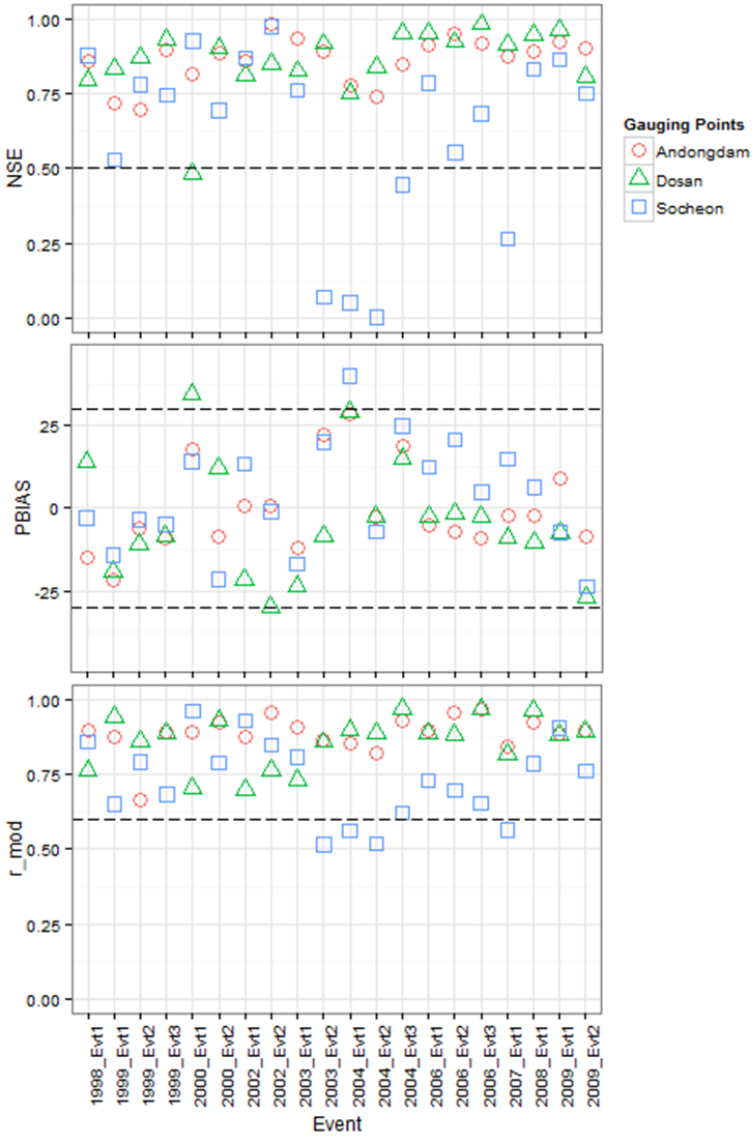

873

874 **Figure 3.** Model performance evaluation statistics of NSE, PBIAS, and r_{mod} (r_mod)
875 for three gauged stations over 20 events. Dosan and Socheon catchments are
876 assumed as ungauged catchments. The black dashed lines represent the acceptance
877 boundaries for each performance evaluation statistic: NSE > 0.5, PBIAS±30%, and
878 r_{mod} > 0.6.

Hydrol. Earth Syst. Sci. Discuss., doi:10.5194/hess-2016-194, 2016
Manuscript under review for journal Hydrol. Earth Syst. Sci.
Published: 9 May 2016

Hydrology and Earth System Sciences
Discussions

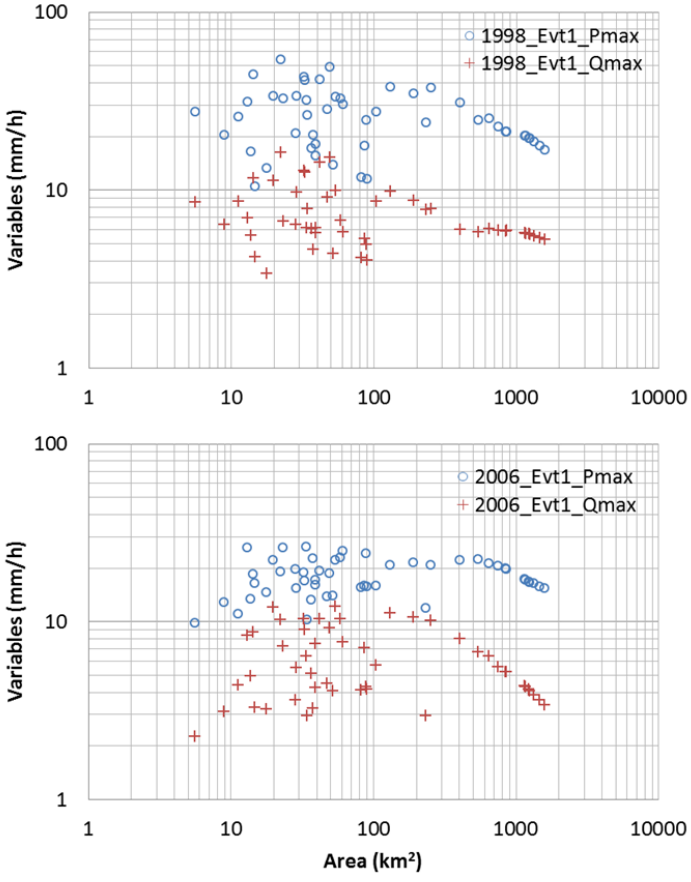

879

880 **Figure 4.** Power law relationship between size of catchments and maximum rainfall

881 (Pmax) or maximum streamflow (Qmax) for two events.

882

883

Hydrol. Earth Syst. Sci. Discuss., doi:10.5194/hess-2016-194, 2016
Manuscript under review for journal Hydrol. Earth Syst. Sci.
Published: 9 May 2016

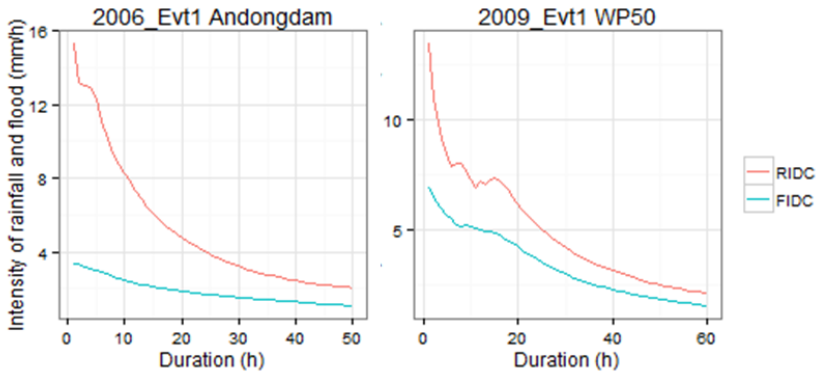

884

885 **Figure 5.** Plot of RIDC and FIDC at the Andongdam gauging point (outlet of the
886 entire catchment) for the 2006 event1 (left hand side) and at the watch point no. 50
887 (the most upper catchment) for the 2009 event1 (right hand side).

888

889

Hydrol. Earth Syst. Sci. Discuss., doi:10.5194/hess-2016-194, 2016
Manuscript under review for journal Hydrol. Earth Syst. Sci.
Published: 9 May 2016

Hydrology and Earth System Sciences
Discussions
Open Access
EGU

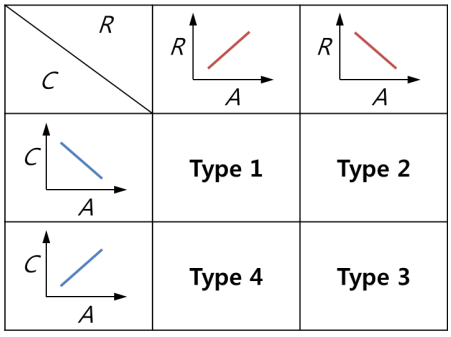

890

891 **Figure 6.** Classification of event type using runoff coefficient (*C*) and
892 rainfall-intensity-ratio (*R*).

893

894

Hydrol. Earth Syst. Sci. Discuss., doi:10.5194/hess-2016-194, 2016
Manuscript under review for journal Hydrol. Earth Syst. Sci.
Published: 9 May 2016

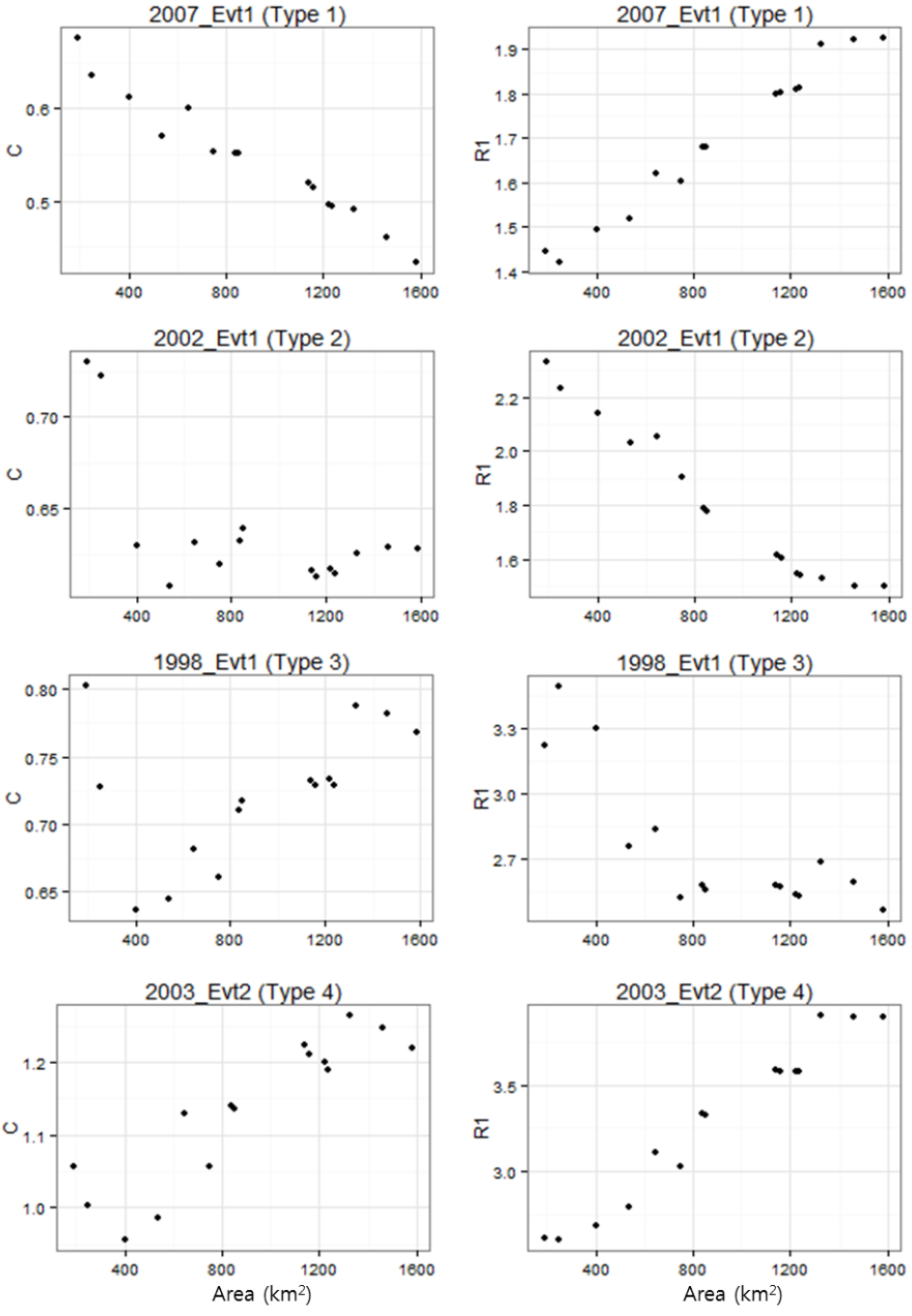

Figure 7. Plot of *C* and $R1$ versus the size of catchments.

Hydrol. Earth Syst. Sci. Discuss., doi:10.5194/hess-2016-194, 2016
Manuscript under review for journal Hydrol. Earth Syst. Sci.
Published: 9 May 2016

Hydrology and Earth System Sciences
Discussions
Open Access
EGU

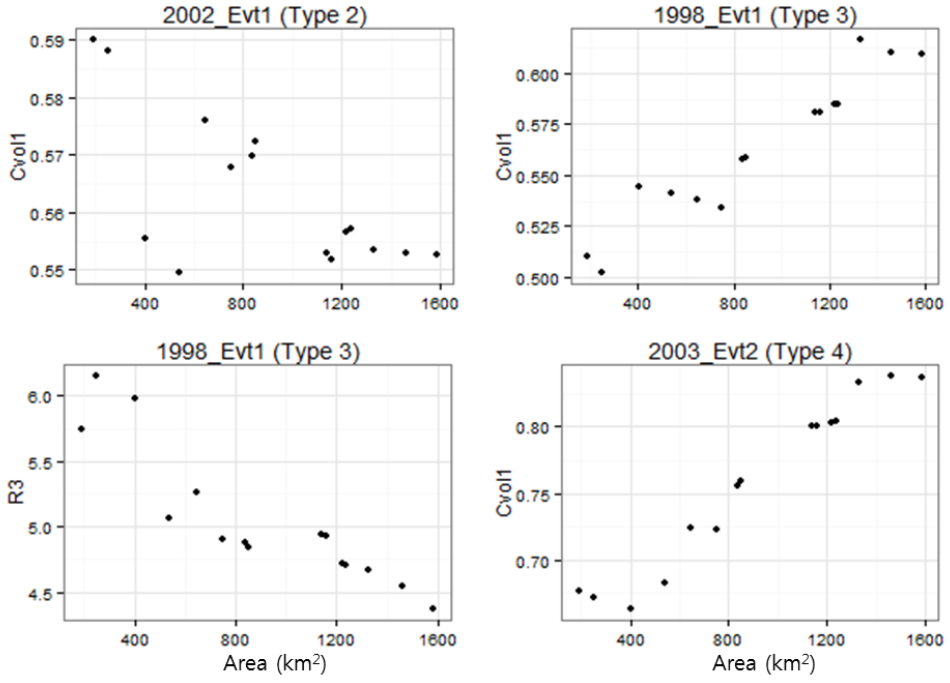

897

898 **Figure 8.** Plot of C_{vol1} and $R3$ versus the catchment size.

899

900

Hydrol. Earth Syst. Sci. Discuss., doi:10.5194/hess-2016-194, 2016
Manuscript under review for journal Hydrol. Earth Syst. Sci.
Published: 9 May 2016

Hydrology and Earth System Sciences
Discussions

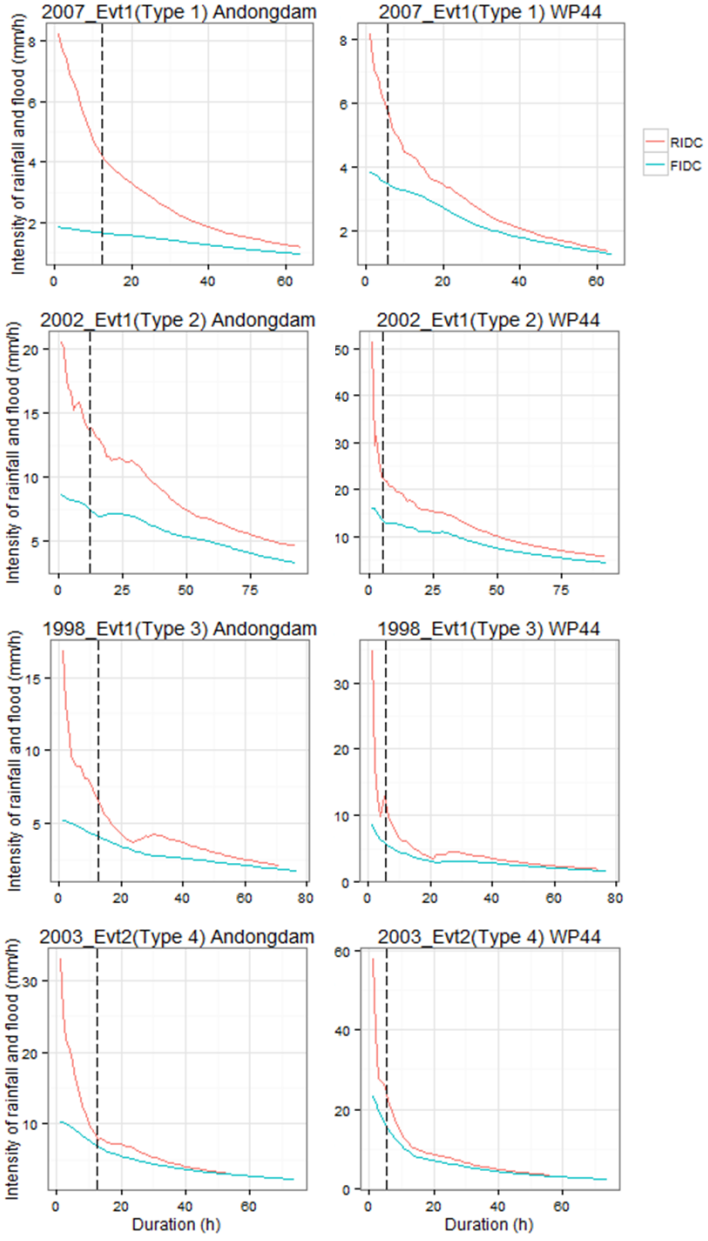

901

902 **Figure 9.** Plots of RIDC and FIDC of very lower and upper catchments for the four
903 types. Vertical black long dashed line represents the time of concentration for these
904 catchments.

Hydrol. Earth Syst. Sci. Discuss., doi:10.5194/hess-2016-194, 2016
Manuscript under review for journal Hydrol. Earth Syst. Sci.
Published: 9 May 2016

Hydrology and Earth System Sciences
Discussions

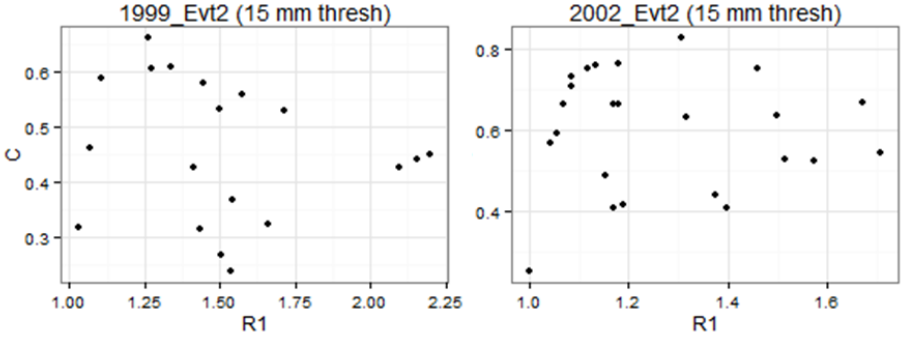

905

906 **Figure 10.** Events with the worst correlations between C and $R1$ for the
907 independent catchments having larger than 15 mm of I_{Tc} value.

908

909

Hydrol. Earth Syst. Sci. Discuss., doi:10.5194/hess-2016-194, 2016
Manuscript under review for journal Hydrol. Earth Syst. Sci.
Published: 9 May 2016

Hydrology and Earth System Sciences
Open Access
Discussions

910 **Table 1.** Description of the parameters in the GRM model.

No.	Parameter	Unit	Range	Description	Calibration
1	IniSaturation	-	0-1	Initial soil saturation ratio	Yes
2	MinSlopeLdSrf	-	0.0001-0.04	Minimum slope of land surface	Yes
3	MinSlopeChBed	-	0.001-0.04	Minimum slope of channel bed	Yes
4	MinChBaseWidth	m	-	Minimum channel width	Yes
5	ChRoughness	-	0.025-0.15	Channel roughness coefficient	Yes
6	IniFlow	CMS	-	Initial stream flow	No
7	DryStreamOrder	-	0-max. str. order	Initial dry stream order	No
8	CalCoefLCRoughness	-	0-4	Land cover roughness coefficient	No
9	CalCoefPorosity	-	0-4	Soil porosity	No
10	CalCoefWFSuctionHead	-	0-4	Soil wetting front suction head	No
11	CalCoefHydraulicK	-	0-4	Soli hydraulic conductivity	No
12	CalCoefSoilDepth	-	0-4	Soil depth	No

911

912

Hydrol. Earth Syst. Sci. Discuss., doi:10.5194/hess-2016-194, 2016
Manuscript under review for journal Hydrol. Earth Syst. Sci.
Published: 9 May 2016

Hydrology and Earth System Sciences
Discussions

913 **Table 2.** Correlation coefficients between runoff coefficients and
914 rainfall-intensity-ratios.

Event	C, $R1$	C, $R1 \bullet R2$	C / C_{vol1}, $R1$	C / C_{vol1}, $R1 \bullet R2$	Type
1999_Evt2	-0.177	-0.187	**0.691**	0.554	1
1999_Evt3	0.425	-0.038	-0.178	**-0.806**	1
2000_Evt2	0.727	0.603	0.591	**0.857**	1
2002_Evt2	-0.015	0.124	**0.812**	0.616	1
2004_Evt1	**0.911**	0.772	-0.708	-0.748	1
2004_Evt2	0.926	0.798	**0.937**	0.893	1
2004_Evt3	0.580	0.474	0.593	**0.824**	1
2006_Evt1	**-0.720**	-0.528	0.381	-0.305	1
2009_Evt1	0.345	**0.755**	0.345	0.375	1
2009_Evt2	0.519	0.530	**0.599**	0.507	1
1999_Evt1	**0.599**	0.365	0.540	0.253	2
2002_Evt1	**0.426**	0.384	0.261	0.363	2
2006_Evt2	0.734	0.723	**0.806**	0.705	2
1998_Evt1	**0.910**	0.801	0.841	0.662	3
2008_Evt1	0.274	0.176	**0.382**	0.280	3
2003_Evt2	0.772	**0.799**	0.747	0.611	4
No. 1st corr.	5	2	6	3	-
No. 2nd corr.	5	4	3	4	-
Total	10	6	9	7	-

915